Differential Imaging Using Fluorescence, Polarization and Spectrum Modulation

Kaoru Yamashita[1*], Takayuki Kimura[1], Ikki Kimura[2],
Yoshihiro Hamakawa[2] and Masanori Okuyama[1]

[1]Graduate School of Engineering Science, Osaka University
1–3, Machikaneyama-cho, Toyonaka, Osaka 560–8531, Japan
[2]Faculty of Engineering, Ritsumeikan University
1–1–1 Noji-higashi, Kusatsu, Shiga 525–0058, Japan

A differential imaging system using fluorescence, polarization and spectrum modulation has been developed. The fluorescent system can provide clear images even in a normal bright room by subtracting a normal image from an image obtained under ultraviolet light irradia tion. Polarization-controlled images can be provided from the difference between images taken with differential polarization of light using a liquid crystal filter. Transparent images and reflection images on a glass window are selectively obtained. Spectrum-differential images have been also acquired using a variable interferometer. The system reveals characteristic spectral images of objects, and the mechanism of wavelength-differential imaging has been confirmed by spectral simulations.

1.   Introduction

Recently, much attention has been focused on various image sensing systems from the viewpoint of high-quality recognition and information processing. Convenient and intelligent imaging techniques are required particularly in the fields of medical and biological engineering, remote sensing, quality control for food products and monitoring systems for environmental pollution. Conventional technology for such imaging currently employs spectral imaging systems such as a multispectral camera with a spectrometer,[1,2] a multi-spectral imager[3] using Fourier transformations and remote sensing systems for environmental measurement mounted on airplanes or satellites.[4] However, conventional systems for sensing require precise control of the optical system and very complicated processes for

---

*Corresponding author, e-mail address: yamashita@ee.es.osaka-u.ac.jp

spectrum alignment and also have rather low spatial resolution or very large volume. The authors have developed a wavelength-differential imaging system for easy processing of two-dimensional spectral images and animation in small and simple devices.[5]

In this work, we extend the system to fluorescent-modulation imaging and polarization controlled imaging and show the characteristic images extracted with the extended system. A numerical simulation of spectral modulation has been carried out and a quantitative evaluation of wavelength-differential imaging is described.

2. Modulated Differential Imaging System

Figure 1 illustrates the modulated differential imaging system. The system can provide modulated images using a conventional color CCD camera with one attachment; an ultraviolet light source for fluorescent modulation imaging, a liquid crystal filter for polarization-controlled imaging or a variable interferometer for spectral modulation imaging. The replaceable modulator attachments are selected according to modulation synchronized with image acquisition. The differential image is obtained by taking the difference between the intensities of the corresponding pixels of two successive images having different degrees of modulation. The image processing of 512×512 pixels for one differential image takes approximately 16 ms. The operating speed of all the attachments is less than 100 ms, so the system can provide an animation of differential images at a frame rate of around 10 frames/s.

3. Fluorescent-Modulation Imaging

Fluorescent-modulation imaging realizes remarkable fluorescent images, even under normal ambient lighting, by subtracting the normal image from an image obtained under
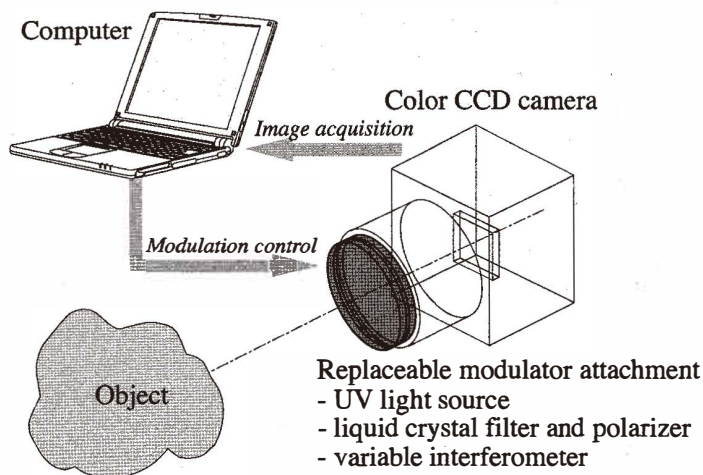
Fig. 1.   Schematic illustration of a modulated differential imaging system.

ultraviolet irradiation. A commercial 15 W black light was used as an excitation source and a band-pass filter was used to suppress visible light intensity from the black light. The main wavelength of the band-pass filter was 355 nm, and the full width at half maximum (FWHM) of the pass band was 53 nm. The black light was driven with an inverter at 1 kHz to avoid interference because commercial electric power frequency of 60 Hz is the first harmonic of the video frame rate at 30 Hz. The light source was controlled with a solid-state relay to blink synchronously with the image acquisition.

Figure 2 shows the result of the fluorescent imaging of a seal using fluorescent ink printed on a one thousand yen bill. Figures 2(a) and 2(b) show the normal image and the image obtained under ultraviolet irradiation, respectively. The fluorescence of the seal cannot be observed in Fig. 2(b) due to ambient lighting being of much higher intensity than
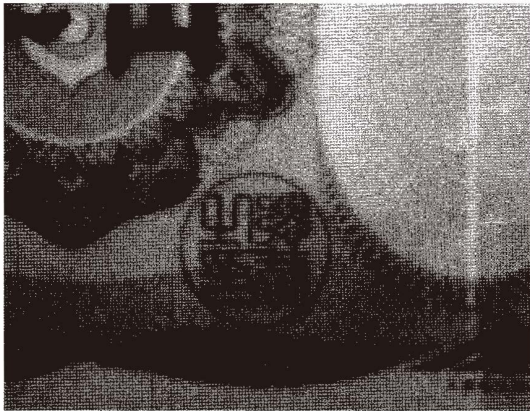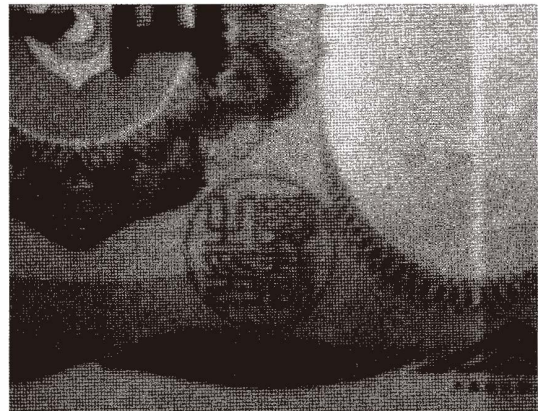
(a)   (b)
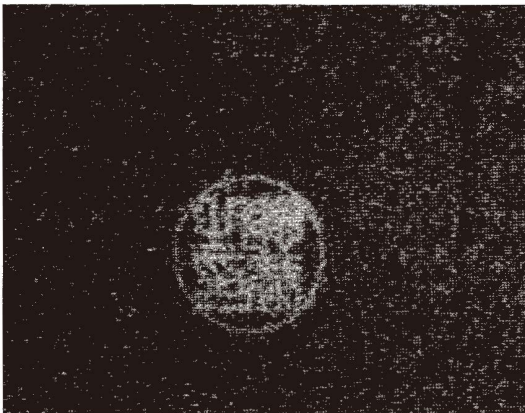
(c)

Fig. 2. Fluorescence-modulation imaging of a bill. (a) normal image, (b) image obtained under UV irradiation , and (c) differential image.

the fluorescence. Figure 2(c) shows the differential image of Figs. 2(a) and 2(b), and the yellow fluorescence of the seal can clearly be observed.

Figure 3 shows the result of the fluorescent imaging of chlorophyll. Mashed parsley was immersed in a small bottle of ethyl alcohol to release chlorophyll. Chlorophyll cells detached from leaf tissue have a fluorescence spectrum with a peak at 680 nm that spreads broadly to the infrared region. Fluorescence cannot be confirmed in Fig. 3(b) under irradiation of ultraviolet light, but the differential image of Fig. 3(c) shows a clear red fluorescence image of the chlorophyll in the alcohol.

4. Polarization-Controlled Imaging

Polarization-controlled imaging separates the transmission and reflection image components from an image on a glass surface that is the superimposition of the transmission

(a)   (b)

(c)
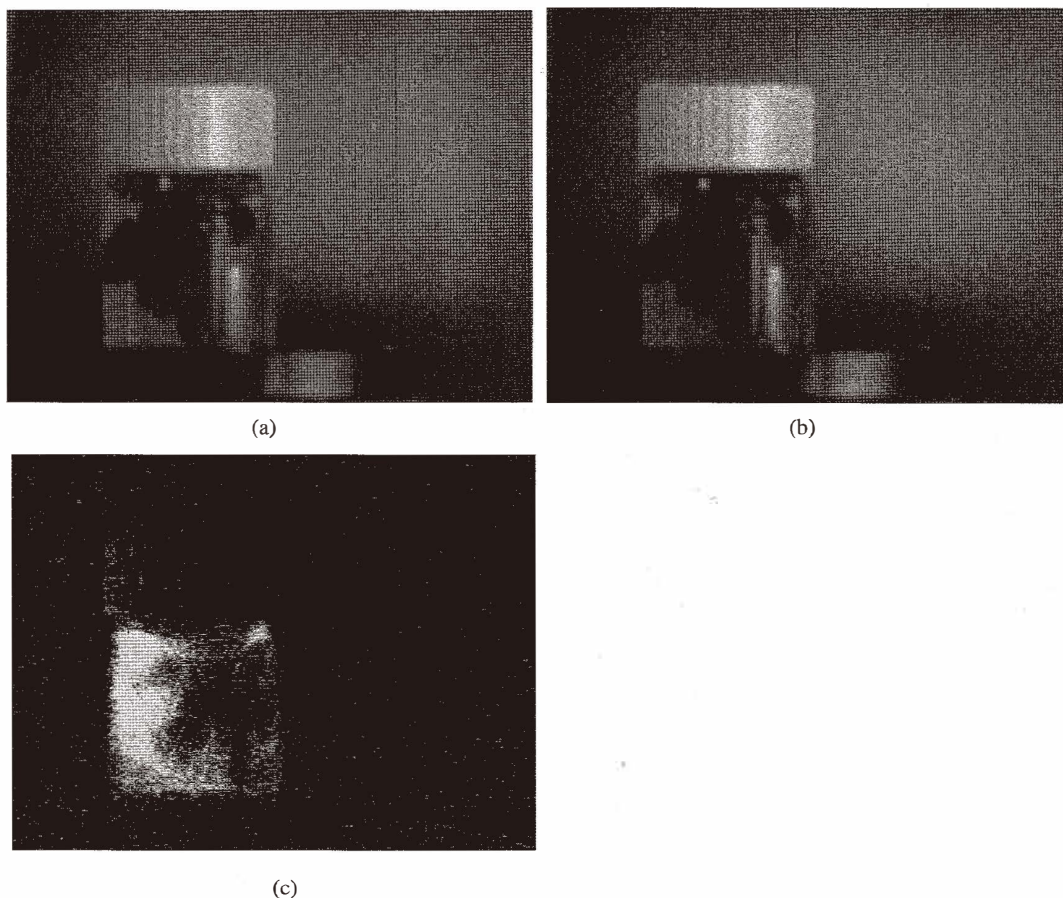
Fig. 3.   Fluorescence-modulation image of chlorophyll. (a) normal image, (b) image obtained under UV irradiation and (c) differential image.

and reflection image components. Because the light incident at the Brewster angle has no parallel polarization component in its reflection, the transmission image component is obtained by cutting the perpendicular polarization component using a polarizer. The reflection image component is obtained by subtracting the transmission image component from the original image. The attachment for polarizationcontrolled imaging consists of a liquid crystal cell enclosing a nematic liquid crystal and a polarizer plate with a polarization effciency of 95%. The cell was rubbed to align the liquid crystal in one direction and has transparent electrodes set on it. The polarization direction can be set to 90 degrees by applying 5 V at a frequency up to 30 Hz.

Figures 4(b) and 4(c) show a polarization-controlled image of two persons on a glass window. Figure 4(a) shows the normal image with no voltage applied to the liquid crystal cell. Neither person can be distinguished in the image. Figure 4(b) shows the transmission image component of the image obtained by applying 5 V to the cell. The person on the

(a)   (b)

(c)
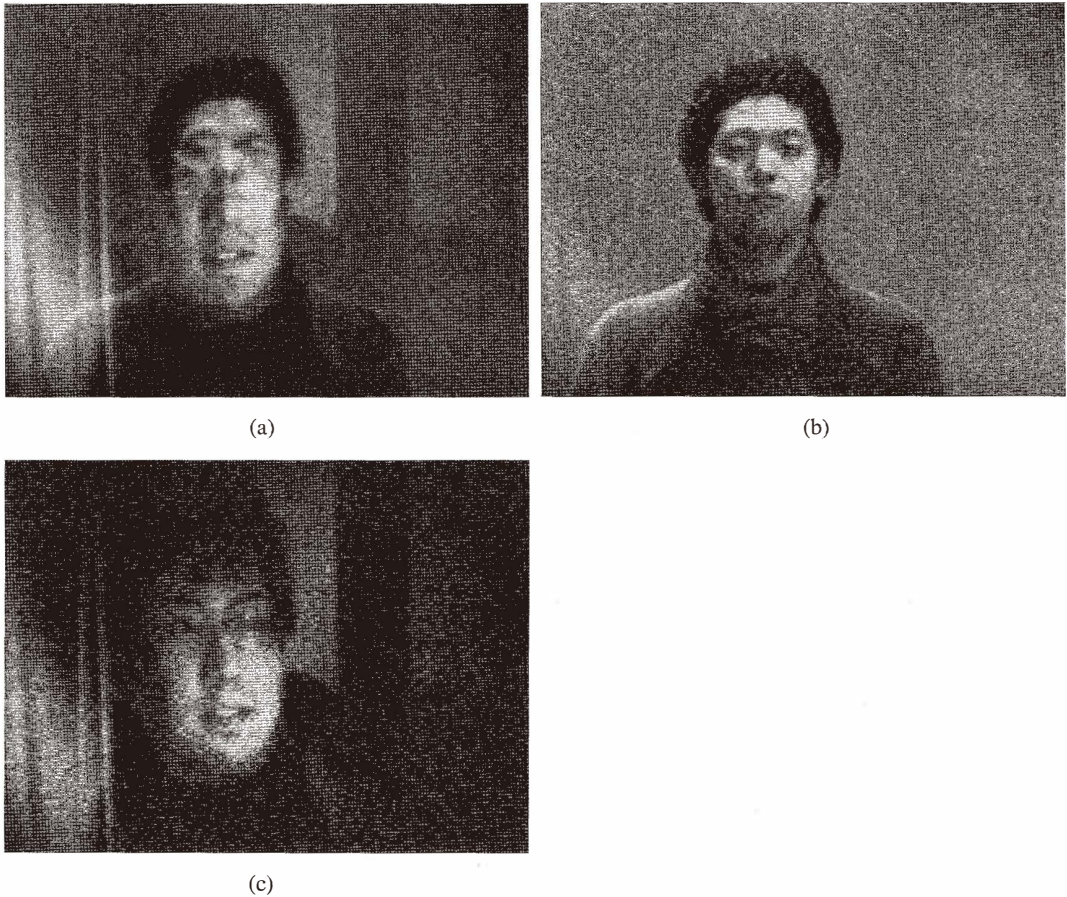
Fig. 4. Polarization-modulation image of two persons through a glass window. (a) normal image, (b) polarized image (transmission image component) and (c) differential image (reffection image component).

other side of the window can be clearly observed. Figure 4(c) shows the reflection image component of the image obtained by subtracting the image shown in Fig. 4(b) from that shown in Fig. 4(a). The image of the person reflected in the window is clearly obtained.

5.   Differential-Wavelength Imaging and Its Numerical Simulation

The differential-wavelength imaging technique extracts a characteristic spectral image as the difference between two images with different transmission spectra taken using a variable filter. The variable filter in this system is a Fabri-Perot interferometer, the transmission spectra of which changes as a function of the gap between two semitranspar-ent substrates controlled with piezoelectric actuators. The authors have reported images corresponding to the spectral differentiation of objects using the fringe shift of the spectrum of the variable interferometer.[5] Figure 5(a) shows a normal image of gerbera, and Fig. 5(b) shows an image superposed on that shown in Fig. 5(a) by wavelength-

(a)

(b)

(c)
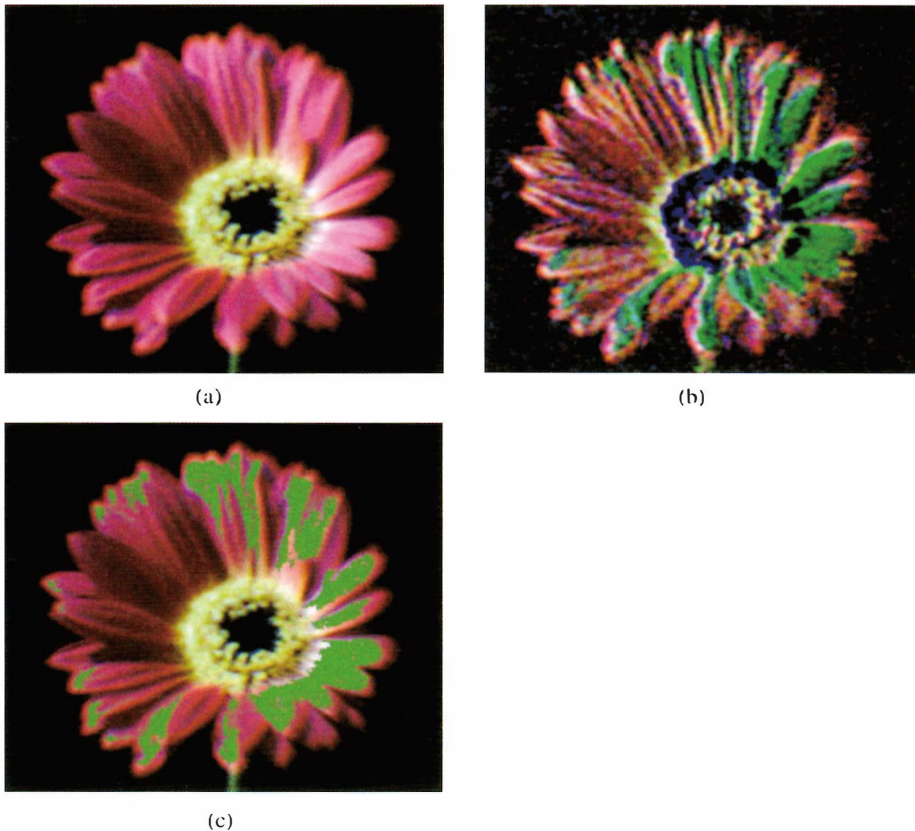
Fig. 5.   Spectrum-modulation image of gerbera. (a) normal image, (b) spectral differential image superimposed on the normal image, and (c) image from simulation.

differential imaging using a variable interferometer. The differential image of Fig. 5(b) shows a remarkable green patterns on many pink petals.

The quantitative simulation of wavelength-differential imaging is described in this section with reference to the gerbera images shown in Fig. 5. The reflectance spectrum $r(\lambda)$ of a gerbera petal is shown in Fig. 6. It has an abrupt slope between 500 nm and 600 nm and has a plateau of relatively high reflectance above 600 nm which corresponds to the pink color of the petals shown in Fig. 5(a). Figure 7 shows two transmission spectra $t_v(\lambda)$ ($V = 0$ and 50) of the variable interferometer with applied voltages of 0 V and 50 V to the piezoelectric actuators. The spectral intensity on the CCD elements in the camera is expressed as the product

$$r_v'(\lambda) = t_v(\lambda)r(\lambda), \tag{1}$$

as shown in Fig. 8. The sensitivities $S_c(\lambda)$ ($C = $ R, G, B) for the red, green and blue colors of the CCD pixels are shown in Fig. 9. Finally, the output voltage $v_{c,v}$ of each pixel of the CCD which takes the image of the gerbera through the interferometer is expressed as

$$v_{c,v} = \int S_c(\lambda)r_v'(\lambda)d\lambda \tag{2}$$

$$(C = \text{R, G, B} \quad V = 0 \text{ and } 50),$$

as shown in Fig. 10.

The brightness b_c of the red, green and blue color for each pixel of the wavelength
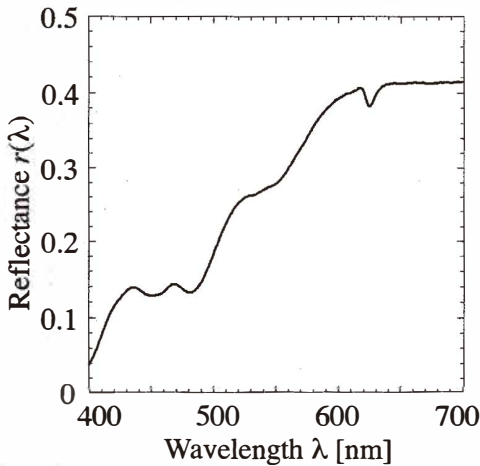
Fig. 6. Reflection spectrum of gerbera petal.
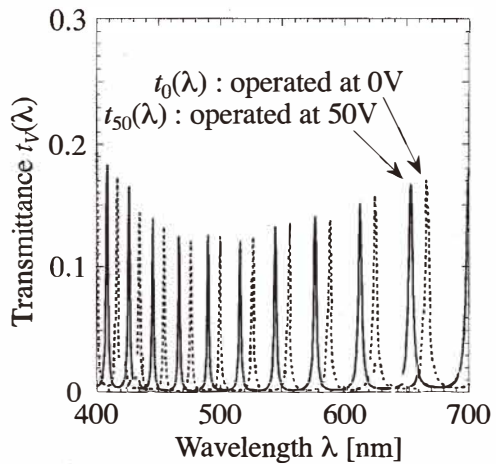
Fig. 7. Transmission spectra of variable interferometer.
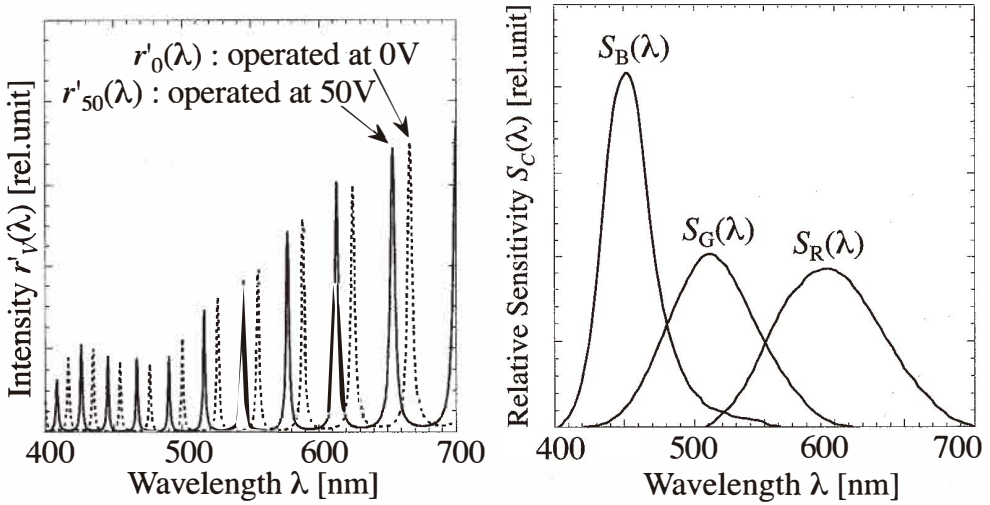
Fig. 8(left).   Spectra predicted on CCD pixels from gerbera through the variable interferometer.
Fig. 9(right).   RGB sensitivities of CCD camera.
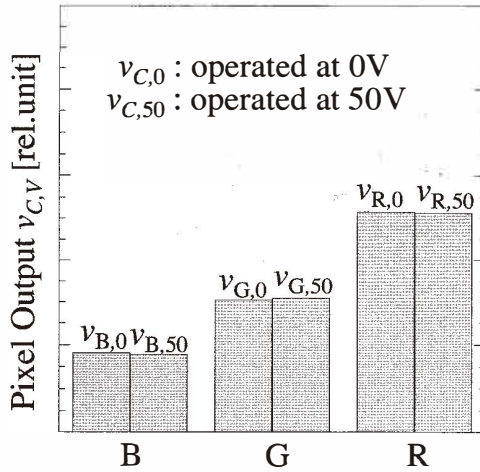
Fig. 10.   RGB output from a pixel in the gerbera petal image through the interferometer.

differential image is expressed as

$$b_c = \left| v_{c,0} - v_{c,50} \right|, \tag{3}$$

as shown in Fig. 11. A green color is composed of the values b_B, b_G and b_R. This color corresponds to the wavelength region from 500 nm to 550 nm where the reffectance of the

gerbera changes sharply as shown in Fig.6. Figure 5(c) show the simulated image superimposed on the normal image. The green colored region on the petal in the simulated image is properly reconstructed in comparison with the real image, Fig. 5(b).

6. Conclusions

A modulation differential imaging system which can be used conveniently to produce fluorescent images, polarization-controlled images and wavelength-differential images has been developed. Fluorescent images of a seal on a bill and chlorophyll are clearly obtained under normal ambient lighting in the form of an image created from the difference between the normal image and the image obtained under ultraviolet irradiation. Polarization-controlled imaging distinguishes between the transmission and reflection image components of superimposed images on a glass window by defining a differential image between the original image and the polarized image using a liquid crystal cell and a polarizer plate. A numerical simulation of wavelength-differential imaging has been carried out on an image of gerbera. The simulated image, which is reconstructed taking into account the reflection spectrum of gerbera, the transmission spectra of the interferometer and the sensitivity spectra of CCD pixels, fits the real image well.

Acknowledgments
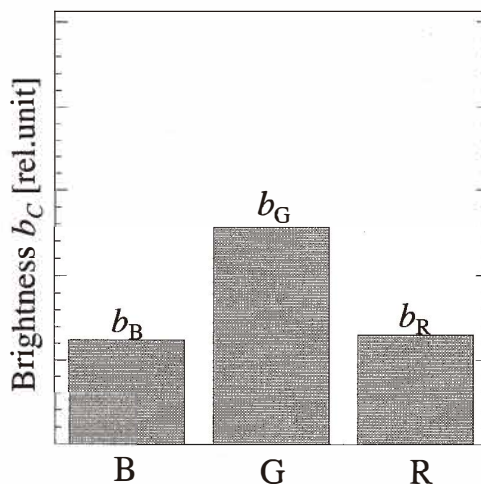
Fig. 11. Difference of RGB outputs from a pixel through the filter operated at 0 V and 50 V.

References

1   E. Preston, T. Bergman, R. Gorenflo, D. Hermann, E. Kopala, T. Kuzma, L. Lazofson and R. Orkis: IEEE AES System Magazine (1994) 13.
2   H. Okamura and F. Masaki: J. Geomag. Geoelectr. **44** (1992) 193.
3   T. Mori, K. Notsu, Y. Tohjima and H. Wakita: Geophysical research letters **20** (1993) 1355.
4   R. Furrer, A. Barsch, C. Olbert and M. Schaale: Geojournal **32** (1994) 7.
5   K. Yamashita, T. Nagashima, S. Hatta, R. Kajihara, Y. Hamakawa and M. Okuyama: Sensors and Actuators A **97** (2002) 177.

About the Authors

Kaoru Yamashita was born in Kyoto, Japan, in 1967, and received his Ph.D. from Osaka University in 2002. He has been a research associate at Osaka University since 1994 and is currently working in the field of micr-mechanical devices and modulation imaging technology.

Takayuki Kimura was born in Osaka, Japan in 1978, and received a bachelor's degree in cngincering from Osaka University in 2002. He studied on fluorescence modulation imaging and polarization-controlled imaging.

Ikki Kimura was born in Osaka, Japan, in 1978, and received a master's degree in engineering from Ritsumeikan University in 2004. He studied on spectralmodulation imaging technology.

Yoshihiro Hamakawa was born in Kyoto, Japan, in 1922, and received his Ph.D. from Osaka University in 1964. He has been a professor at Ritsumeikan University and an emeritus professor of Osaka university since 1996, the vice chancellor of Ritsumeikan University from 1997 to 2000, and the advisory professor to the Chancellor of Ritsumeikan University since 2003. He is currently working in the field of amorphous silicon and related materials and their applications for solar cells and light emitting devices.

Masanori Okuyama was born in Osaka, Japan, in 1946, and received his Ph.D. from Osaka University in 1973. He has been a professor at Osaka University since 1991 and is currently working in the field of silicon surfaces, silicon dioxide and its interface with silicon, ferroelectric thin films and their application to functional devices such as memory and sensors.